Temperature-Dependent Recombination Processes in Small-Sized PbSe/PbS Core/Shell Colloidal Quantum Dots

Diana YANOVER, Anna RUBIN-BRUSILOVSKI, Richard K. ČAPEK, Aldona SASHCHIUK *, Efrat LIFSHITZ

Schulich Faculty of Chemistry, Russell Berrie Nanotechnology Institute and Solid State Institute, Technion - Israel Institute of Technology, Haifa 32000, Israel

The work focuses on the optical investigation of temperature-dependent recombination processes in small-sized PbSe/PbS core/shell colloidal quantum dots (CQDs) with core diameter of $(2-2.5)$ nm and the shell thickness of $(0.5-1.0)$ nm under air-free conditions and after air exposure. These CQDs have a tunable absorption edge around 1 μm and a rather narrow photoluminescence linewidth, their emission recombination process is characterized by the μs time-scale and by longer radiative lifetimes in the entire temperature range and especially at low temperatures (a 2.6-fold increase) as compared to the corresponding PbSe samples. The PbSe/PbS core/shell CQDs are oxidation-stable towards time-limited air exposure.

Keywords: small-sized CQDs, PbSe/PbS core/shell, surface oxidation, temperature-dependent PL, and PL dynamics.

1. INTRODUCTION

IV–VI (PbTe, PbSe, PbS) colloidal quantum dots (CQDs) are very attractive materials from the scientific and technological points of view due to their unique electronic and optical properties associated with strong quantum confinement and to the possibility of their applications in near infra-red (NIR) lasers, solar cells, and nano-electronic devices.

Besides the achievements in the synthesis and applicational development of various IV-VI CQDs, their properties have been studied extensively in different environments (air or inert). It was shown that air-exposed PbS CQDs demonstrate the *p*-type mobility, in contrast to the *n*-type mobility in pristine PbS CQDs [1]. Both PbSe and PbS CQDs show a reduction in the photoluminescence (PL) intensity when exposed to air [2]. Various approaches, including hybrid passivation and exchange of surface ligands for controlling the surface covering, were proposed to stabilize the CQD surface against oxidation. Efficient passivation of PbSe CQDs is achieved by the epitaxial growth of a PbS shell onto PbSe CQDs, leading to the formation of a core/shell structure [3]. Recently, high quality small-sized PbSe/PbS core/shell CQDs with band-gap energy (E_g) of $(1.3-1.0)$ eV were produced. PbS and PbSe have similar crystallographic and dielectric parameters and thus they form a perfect crystalline heterostructure. Hybrid passivated PbS and small-sized PbSe/PbS CQDs-based solar cells show power conversion efficiency of 7 % [4] and 4 % [5], respectively.

The present study of thermally activated PL emission and excited-state lifetime in small-sized PbSe/PbS core/shell CQDs was motivated by the fact that, currently, their fundamental properties, including the influence of

oxygen on radiative processes, are being extensively investigated. Here we show that the exposure of PbSe/PbS core/shell CQDs to air for a limited time (up to 20 min), in contrast to PbSe CQDs, does not quench their PL emission. The temperature dependences of the integrated PL intensity (I_{PL}) and of the radiative lifetime suggest that PL quenching processes occur via the mechanism of phonon-assisted dark-to-bright activation.

2. EXPERIMENTAL

The synthesis and characterization of ultra-small PbSe CQDs of $(2-2.5)$ nm in diameter and of small-sized PbSe/PbS core/shell CQDs with the overall diameter of $(3.0-3.5)$ nm and E_g in the range of $(1.0-1.4)$ eV were described previously [6]. Optical absorption spectra of the CQDs were recorded in tetrachloroethylene at room temperature (RT). To perform continuous-wave (cw-) and time-resolved (tr-) PL measurements, the CQDs were embedded in 2,2,4,4,6,8,8-heptamethylnonane, a glass-forming solvent at low temperatures. The samples were inserted in a Janis variable-temperature cryogenic system.

3. RESULTS AND DISCUSSION

Thermally activated processes in the CQDs were studied by following the variation of the emission spectra with temperatures (T) under air-free conditions and after air exposure. The optical absorption spectra measured at RT and the cw-PL spectra measured at various T, ranging from 5 K to 290 K, under air-free conditions are shown in Fig. 1, a – b. Ultra-small (2.2 nm in diameter) PbSe and 3.4 nm in diameter (2.2 nm core) core/shell PbSe/PbS CQDs were used. It can be seen that the absorption and emission spectra of PbSe/PbS core/shell CQDs are red-shifted as compared to the corresponding PbSe cores. Namely, the E_g values of PbSe/PbS CQDs at RT are centred around 1.4 eV, while those of PbSe CQDs are centred around 1.6 eV.

---

*Corresponding author. Tel.: +972-4-8295644; fax.: +972-4-8295703.
E-mail address: *chaldona@tx.technion.ac.il* (A. Sashchiuk)
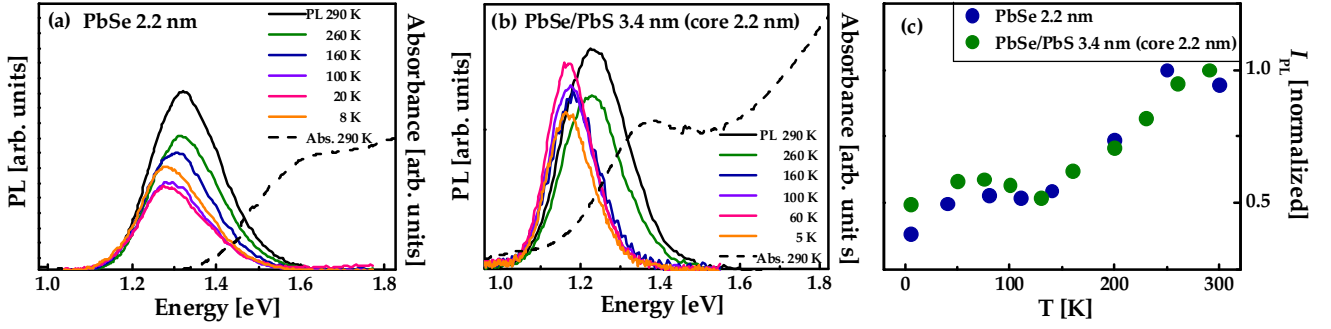
Fig. 1. Optical absorption (dashed black lines) and cw-PL emission spectra (solid lines) of (a) 2.2 nm PbSe CQDs; (b) 3.4 nm PbSe/PbS core/shell CQDs with the core diameter of 2.2 nm; (c) integrated PL intensity at various temperatures of the CQDs presented in (a) and (b). All measurements were performed in the air-free environment

The PL and absorption spectral linewidth are comparable, which suggests that the large PL spectral linewidth is the consequence of inhomogeneous broadening due to the distribution of particle sizes.

The Stokes shift (the energy shift between the first absorption and emission bands) in PbSe/PbS CQDs (see Fig. 1, b) is ~ 140 meV at RT, which is about only half of the value (~ 300 meV) observed in the initial PbSe CQDs (Fig. 1, a). The exceptionally large Stokes shift in ultra-small PbSe CQDs is, probably, due to the intervalley splitting, which originates from the structural anisotropy of the ultra-small nanoparticles, observed in the high-resolution transmission electron images of the CQDs (not shown here). The other possible contributions to the large Stokes shift in ultra-small PbSe CQDs are discussed elsewere [6].

The spectra presented in Fig. 1, a–b, show the PL emission evolution with temperature for both the core and core/shell samples. Namely, the PL energy peak is shifted, the PL band linewidth and the integrated PL intensity (I_{PL}) are changed. The temperature increase causes a PL blue shift (to higher energy), which is, mainly, due to lattice dilation and electron-phonon coupling [7]. Additionally, with increasing temperature, PL linewidth increases as a result of homogeneous broadening, which occurs due to the exciton scattering by optical and acoustic phonons. It can be seen that the PL linewidth in PbSe/PbS CQDs is relatively narrow as compared to those of PbSe CQDs in the entire temperature range. This is accounted for by the narrower nanoparticle size distribution in the core/shell CQDs. The ultra-small PbSe CQDs have a relatively broad size distribution (~ 15 %) because the quenching reaction occurs close to the nucleation event and, thus, prior to the size focusing.

The plot of I_{PL} vs T for the PbSe and PbSe/PbS CQDs used in experiments (a) and (b) is presented in Fig. 1, c. The values of $I_{PL}(T)$ were calculated by integrating the PL band intensities. The I_{PL} value at each temperature was normalized by the maximal value obtained at RT. There is a moderate increase of $I_{PL}(T)$ between 5 K and 70 K, which is due to the phonon activation of the optically inactive dark state. Then, at temperatures >140 K and up to RT, the PL intensity increases significantly due to the phonon-assisted exciton spin-flip (dark-to-bright thermal activation). Thus it can be concluded that the maximal PL emission intensity at RT corresponds to electron-hole radiative recombination from a bright-exciton state.

The temperature-dependent PL emission spectra of PbSe CQDs exposed to air for 20 min are presented in Fig. 2, a. The cw-PL emission of the PbSe CQDs drops with increasing T. Such a drastic effect of air exposure on I_{PL} may be associated with thermally-activated trapping into oxidation-induced shallow-trap states on the CQD surface at elevated temperatures.

The dependences of normalized I_{PL} on T for the PbSe/PbS core/shell CQDs that were air-exposed for (20–200) min are shown in Fig. 2, b. It is evident that exposure for a limited time (20 min) does not lead to dramatic changes of I_{PL}. Air-exposure for a longer time results in oxidation, which is acompanied by the loss of surface Pb atoms and oleic acid ligands with subsequent quenching of the PL emission intensity.
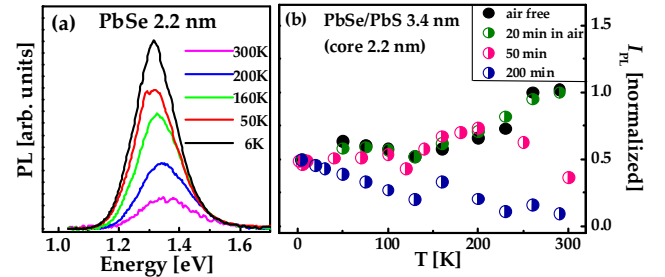
Fig. 2. (a) cw-PL emission spectra of PbSe CQDs (2.2 nm in diameter) air-exposed for 20 min; (b) Normalized I_{PL} temperature dependences of 3.4 nm PbSe/PbS CQDs (the same as used in the Fig. 1, b, experiment) air-exposed for different periods (20–200 min)

The results of the tr-PL measurements at various T were used to elucidate the nature of the radiative processes and to additionally support the dark-to-bright activation hypothesis. The temporal evolution of the PL spectra was investigated by following the PL emission intensity decay over time after exciting the sample at 1.17 eV. The PL decay curves of 2.2 nm PbSe CQDs recorded under air-free conditions at various T are presented in Fig. 3, a. At high temperatures (160 K – 200 K), the PL decay dynamics is predominantly single-exponential, whereas at low temperatures (4 K – 100 K) the dynamics obeys the two-exponential law: $I(t) = A_1 \exp(-t/\tau_1) + A_2 \exp(-t/\tau_2)$. The PL decay time is measured as $\tau_0 = A_1 \tau_1 + A_2 \tau_2$. It can be suggested that the two recombination processes revealed in ultra-small PbSe CQDs at low temperatures are connected
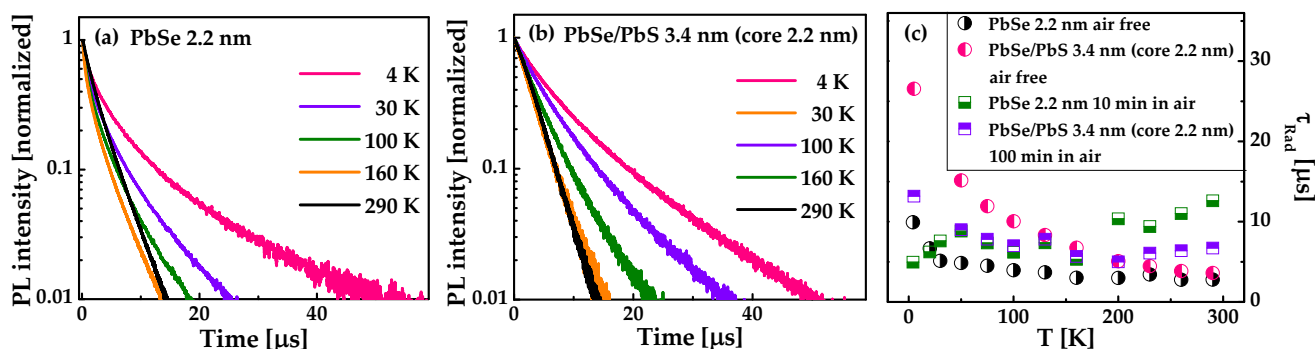
Fig. 3. Representative tr-PL emission curves of (a) PbSe and (b) PbSe/PbS CQDs measured in air-free environment at variuos *T* as indicated in the legend; (c) dependences of τ_{Rad} on *T* for 2.2 nm PbSe and 3.4 nm PbSe/PbS CQDs with/without air exposure

with the dark and deep-trap states. However, in the case of 3.4 nm PbSe/PbS CQDs, the PL decay dynamics is approximately single-exponential in the studied temperature range (Fig. 3, b). The values of τ_0 at each temperature depend on the radiative (τ_{Rad}) and nonradiative (τ_{NRad}) processes according to equation $1/\tau_0 = 1/\tau_{Rad}(T) + 1/\tau_{NRad}(T)$. The I_{PL} and PL quantum efficiency (PL QE, η) are related to each other in the following manner: $\eta(T) = I_{PL}(T)/I_0 = \tau_0(T)/\tau_{Rad}(T)$, where I_0 is the exciting photon flux. The value of η ~ 60 % obtained in our experiments for PbSe and PbSe/PbS CQDs is the maximum efficiency that has been measured for non-oxidized samples at RT.

Radiative lifetime is a meaningful parameter to consider when comparing the behavior of core/shell and core CQDs. The $\tau_{Rad}(T)$ in Fig. 3, c, was determined from measured $\tau_0(T)$ and $I_{PL}(T)$ of PbSe and PbSe/PbS CQDs with/without air exposure. There is a significant difference between the τ_{Rad} temperature dependences for the oxidized and non-oxidized CQDs. Air-free PbSe/PbS CQDs exhibit a strong temperature dependence of τ_{Rad}, which decreases from 26 μs at 5 K to 3.7 μs at 290 K. This effect can result from the elimination of the trapping surface states caused by the growth of the crystalline-matched epitaxial shell, by the quasi-type-II character of the heterostructures, or/and by the total increase of the CQD diameter. The pronounced drop of the τ_{Rad} values for PbSe/PbS CQDs and the mild drop for PbSe CQDs up to 50 K is due to dark-state activation. In the range of (100 – 300) K, τ_{Rad} decreases for PbSe/PbS CQDs as a result of the thermal activation of the bright state. The PL decay dynamics of air-free and air-exposed PbSe and PbSe/PbS CQDs is different. The data presented in Fig. 3, c, show that τ_{Rad} of air-free CQDs reaches its maximum at low *T*, which correlates with low I_{PL}. The temperature dependence of τ_{Rad} in both PbSe and PbSe/PbS CQDs is in accordance with the phonon-asisted dark-bright activation model. The radiative lifetime in air-exposed PbSe CQDs, in contrast to PbSe/PbS CQDs, is maximal at RT. Such behaviour can be explained by the activation of trapping states in PbSe CQDs at RT due to surface oxidation, which influeces the radiative emission process.

4. CONCLUSIONS

The study of cw- and tr-PL at different temperatures shows the effect of PbS passivation on the optical properties of PbSe CQDs. The results indicate that the PbS shell provides protection from fast surface oxidation, thereby preventing the PL emission quenching for at least 20 min of air exposure. The oxidation-induced trapping states influence the radiative process in ultra-small PbSe CQDs. PbSe/PbS CQDs have relatively narrow emission bands, a longer excited-state lifetime at low temperatures, and higher tolerance to oxygen exposure for a limited period of time as compared to the corresponding PbSe CQDs.

REFERENCES

1. **Tang, J., Brzozowski, L., Barkhouse, D., Wang, X., Debnath, R., Wolowiec, R., Palmiano, E., Levina, L., Pattantyus-Abraham, A., Jamakosmanovic, D., Sargent, E.** Quantum Dot Photovoltaics in the Extreme Quantum Confinement Regime: The Surface-Chemical Origins of Exceptional Air- and Light-Stability *ACS Nano* 4 2010: pp. 869 – 878.
http://dx.doi.org/10.1021/nn901564q

2. **Chappell, H., Hughes, B., Beard, M., Nozik, A., Johnson, J.** Emission Quenching in PbSe Quantum Dot Arrays by Short-Term Air Exposure *Journal of Physical Chemistry Letters* 2 2011: pp. 889 – 893.

3. **Brumer, M., Kigel, A., Amirav, L., Sashchiuk, A., Solomesch, O., Tessler, N., Lifshitz, E.,** PbSe/PbS and PbSe/PbSe$_x$S$_{1-x}$ Core/Shell Nanocrystals *Advanced Functional Materials* 15 2005: pp. 1111 – 1116.
http://dx.doi.org/10.1002/adfm.200400620

4. **Ip, A., Thon, S., Hoogland, S., Voznyy, O., Zhitomirsky, D., Debnath, R., Levina, L., Rollny, L., Carey, G., Fischer, A., Kemp, K., Kramer, I., Ning, Z., Labelle, A., Chou, K., Amassian, A., Sargent, E.** Hybrid Passivated Colloidal Quantum Dot Solids *Nature Nanotechnology* 7 2012: pp. 577 – 582.
http://dx.doi.org/10.1038/nnano.2012.127

5. **Etgar, L., Yanover, D., Capek, R.-K., Vaxenburg, R., Xue, Z., Liu, B., Nazeeruddin, M., Lifshitz, E., Gratzel, M.** Core/Shell PbSe/PbS QDs TiO2 Heterojunction Solar Cell *Advanced Functional Materials* 23 2013: pp. 2736 – 2741.
http://dx.doi.org/10.1002/adfm.201202322

6. **Yanover, D., Capek, R.-K., Rubin-Brusilovski, A., Vaxenburg, R., Grumbach, N., Maikov, G.-I., Solomeshch, O., Sashchiuk, A., Lifshitz, E.** Small-Sized PbSe/PbS Core/Shell Colloidal Quantum Dots *Chemistry of Materials* 24 2012: pp. 4417 – 4423.
http://dx.doi.org/10.1021/cm302793k

7. **Olkhovets, A., Hsu, R., Lipovskii, A., Wise, F.** Size-dependent Temperature Variation of the Energy Gap in Lead-salt Quantum Dots *Physical Review Letters* 81 1998: pp. 3539 – 3542.